Research Article/Araştırma Makalesi

GAZİ
JOURNAL OF ENGINEERING SCIENCES

Investigation of Thermomechanical Material Properties of Functionally Graded Sandwich Composite Plates with Metamaterial Honeycomb Core Layer

Kerim Gokhan Aktas[*a]

Submitted: 08.11.2024 Revised: 06.12.2024 Accepted: 17.12.2024 doi:10.30855/gmbd.0705AR12

ABSTRACT

In this article, the thermomechanical properties of a composite sandwich plate with functionally graded (FG) surface layers and a metamaterial honeycomb core layer are investigated under temperature loading. The hexagonal honeycomb core plate is sandwiched between two surface layers with FG stainless steel (SUS304) and zirconia (ZrO2) metal-ceramic matrix. The mechanical and thermal behavior of the core and surface layers changes depending on the temperature. Power law functions and Gibson's equations are employed to specify the equivalent effective material properties of the sandwich plate. Numerical analyses are carried out to investigate the effect of variables such as geometrical parameters of the honeycomb structure, temperature rise and power law parameter on the variation of the thermomechanical material behavior of the sandwich plate. According to the analysis results, it is concluded that the desired thermal and mechanical properties can be tuned by adjusting the honeycomb cell geometric configurations and the material compositions of the FG layers. It is also emphasized that the combination of mechanical and thermal properties in honeycomb structures enables them to perform effectively in demanding environments, where both strength and thermal resistance are required.

Keywords: FG sandwich honeycomb plate, metamaterial, thermomechanical, SUS304, ZrO_2

[a,*] Karabuk University, Engineering Faculty, Dept. of Mechanical Engineering 78100-Karabük, Türkiye
Orcid: 0000-0002-8076-6799
e mail: kerimgokhanaktas@karabuk.edu.tr

*Corresponding author: kerimgokhanaktas@karabuk.edu.tr

Metamalzeme Bal Peteği Merkez Katmanlı Fonksiyonel Derecelendirilmiş Sandviç Kompozit Plakaların Termomekanik Malzeme Özelliklerinin İncelenmesi

ÖZ

Bu makalede, fonksiyonel olarak derecelendirilmiş (FD) yüzey plakalarına ve bir metamalzeme bal peteği merkez plaka katmanına sahip kompozit bir sandviç plakanın termomekanik özellikleri sıcaklık yükü etkisi altında incelenmiştir. Altıgen bal peteği merkez plakası, FG paslanmaz çelik (SUS304) ve zirkonya (ZrO2) metal-seramik matrisli iki yüzey plakası arasına sandviç edilmiştir. Merkez plaka ve yüzey plakaların mekanik ve termal özellikleri sıcaklığa bağlı olarak değişmektedir. Sandviç plakanın eşdeğer etkin malzeme özelliklerini belirlemek için güç yasası fonksiyonları ve Gibson denklemleri kullanılmıştır. Petek yapının geometrik parametreleri, sıcaklık artışı ve güç kanunu parametresi gibi değişkenlerin sandviç plakanın termomekanik malzeme davranışının değişimi üzerindeki etkisini araştırmak için sayısal analizler gerçekleştirilmiştir. Analiz sonuçlarına göre, petek hücrelerin geometrik konfigürasyonlarının ve FG plakalarının malzeme bileşimlerinin ayarlanmasıyla istenen termal ve mekanik özelliklerin ayarlanabileceği sonucuna varılmıştır. Ayrıca, bal peteği yapılardaki mekanik ve termal özelliklerin kombinasyonunun hem mukavemet hem de termal direncin gerekli olduğu zorlu ortamlarda etkili bir şekilde performans göstermelerini sağlayabileceği vurgulanmıştır.

Anahtar Kelimeler: FD sandviç bal peteği plaka, metamalzeme, termomekanik, SUS304, ZrO_2

To cite this article: K. G. Aktas, "Investigation of Thermomechanical Material Properties of Functionally Graded Sandwich Composite Plates with Metamaterial Honeycomb Core Layer", *Gazi Journal of Engineering Sciences*, vol.10, no:3, pp. 645-656, 2024. doi:10.30855/gmbd.0705AR12

1. Introduction

Metamaterials are engineered materials with unique properties that arise from their structure rather than their composition. The integration of metamaterials into sandwich plate designs enhances their mechanical performance, making them suitable for a variety of applications, including aerospace, automotive, and civil engineering. Metamaterials sandwich plates represent a significant advancement in material science, particularly in the fields of acoustics, vibration control, and electromagnetic wave manipulation. In terms of mechanical properties, metamaterials exhibit unique behaviors such as negative Poisson's ratio and non-positive thermal expansion. Negative Poisson's ratio materials expand laterally when stretched, which can be advantageous in applications requiring enhanced energy absorption and structural resilience [1-3]. For example, auxetic mechanical metamaterials have been shown to possess superior energy and acoustic absorption capabilities, making them suitable for applications in vibration control and impact mitigation [4]. The design of metamaterials often involves complex geometrical configurations that allow for tunable mechanical properties. Recent studies have explored hierarchical structures that combine different lattice types to achieve desired mechanical responses, such as enhanced stiffness or flexibility [5-8].

Honeycomb sandwich plates are composite structures that consist of two outer layers and a lightweight core made of honeycomb material. These structures are widely utilized in various engineering applications due to their unique mechanical and thermal properties, including high strength-to-weight ratios, excellent energy absorption capabilities, and good thermal insulation [9,10]. The mechanical properties of honeycombs, such as compressive strength, energy absorption, and stiffness, are influenced by their geometric configurations and material compositions. For instance, the introduction of hierarchical designs in honeycomb structures has been shown to enhance thermal resistance and mechanical performance by allowing for tailored geometric parameters that optimize heat dissipation and structural integrity [5]. One of the significant advantages of honeycomb sandwich plates is their ability to minimize weight while maintaining structural integrity. Research has shown that hexagonal honeycomb cores exhibit lower weight compared to truss lattice cores and monolithic plates, making them an attractive option for applications where weight reduction is critical [9]. Additionally, the dynamic compressive response of honeycomb structures has been extensively studied, revealing that the mechanical properties can be optimized through careful design of the core geometry and material selection [11–13]. For instance, the introduction of auxetic honeycomb structures, which exhibit a negative Poisson's ratio, has been shown to enhance the energy absorption characteristics of sandwich plates under impact loading [14,15]. Thermal properties of honeycomb structures are equally important, especially in high-temperature applications. Research indicates that honeycombs with thicker cores exhibit higher strength and stiffness, which are crucial for maintaining structural integrity under thermal stress [16]. Additionally, the thermal conductivity of honeycomb cores can be optimized through material selection and structural design, allowing for effective thermal management in aerospace applications [17]. The combination of mechanical and thermal properties in honeycomb structures enables them to perform effectively in demanding environments, where both strength and thermal resistance are required.

The incorporation of functionally graded materials (FGMs) within honeycomb structures can further enhance their mechanical properties, allowing for a more controlled response under various loading conditions [18,19]. FGMs are a remarkable subclass of advanced composite materials distinguished by a continuous gradient in composition and properties across their thickness. This gradation facilitates customized mechanical and thermal properties, rendering FGMs especially advantageous in many applications. The thermal properties of FGMs are especially important in applications exposed to high thermal environments [20,21]. The continuous change in thermal conductivity and expansion coefficients enables FGMs to withstand thermal gradients without significant thermal stresses [22,23]. Investigations indicate that FGMs can be designed to demonstrate enhanced thermal insulation or conduction characteristics, based on the specific application demands. The incorporation of FGMs in thermal barrier coatings can markedly enhance thermal resistance of components subjected to elevated temperatures, such as turbine blades in jet engines [24]. The chemical composition of FGMs has been modified to improve their thermal endurance against thermal loads. Duc et al. [25] examined the mechanical and thermal endurance of eccentrically stiffened FG conical shell panels, highlighting the significance of material gradation in enhancing thermal resistance. Zhou et al. [24] investigated the load dispersion in porous metal-ceramic FGMs under thermomechanical load, emphasizing the significance of comprehending the response of these materials to complicated loading circumstances.

According to Chung's [26] study on thermoelastic approaches to FG plates that are subjected to heat mechanical responses are significantly influenced by temperature variations.

The thermal and mechanical characteristics of SUS304 and ZrO_2 are crucial in numerous engineering tasks, especially for FGMs in which both substances are integrated to utilize their beneficial qualities. SUS304 is distinguished for its superior corrosion resistance and mechanical strength, whilst ZrO_2 is esteemed for its elevated thermal endurance and minimal thermal conductivity. When used as a metal-ceramic matrix in FGMs, SUS304 and ZrO2 can generate materials that incorporate the high strength and flexibility of SUS304 with the thermal insulation characteristics of ZrO_2. This combination can provide better potential performance in applications in aerospace and automotive applications where materials are exposed to high thermal loads. Grading in material characteristics can also contribute to decreasing thermal stresses and improving the durability of composites under high thermal environments [24,27].

Investigation of the thermomechanical material behavior of composite sandwich plate with metamaterial honeycomb core and metal-ceramic matrix FG surface layers with temperature dependent parameters is a new and unstudied subject. Because of their exceptional mechanical and thermal qualities, SUS304 and ZrO_2 have been chosen as the matrix substances for the suggested sandwich plate, that can be employed in a variety of scientific and technological areas. The proposed study is anticipated to make a significant contribution to the field of high temperature and corrosion applications in electromechanical systems, aerospace, automotive, and marine applications.

2. Theoretical Formulation

2.1. Model description

A mathematical model of FG sandwich structure with two FG surface layers and honeycomb core layer subjected to temperature load is established, as shown in Figure 1. h_c and h_s refer to the thicknesses of the core layer and FG layers, respectively. The honeycomb core of the sandwich structure consists of hexagonal unit cells in a specific arrangement. Also, as shown in the figure, the sandwich plate is subjected to a temperature load along the z-axis. The hexagonal honeycomb core layer is sandwiched between two FG layers. The material utilized for the honeycomb core is SUS304. In addition, SUS304 and ZrO_2 are considered to be distributed with power law distribution in the surface layers.

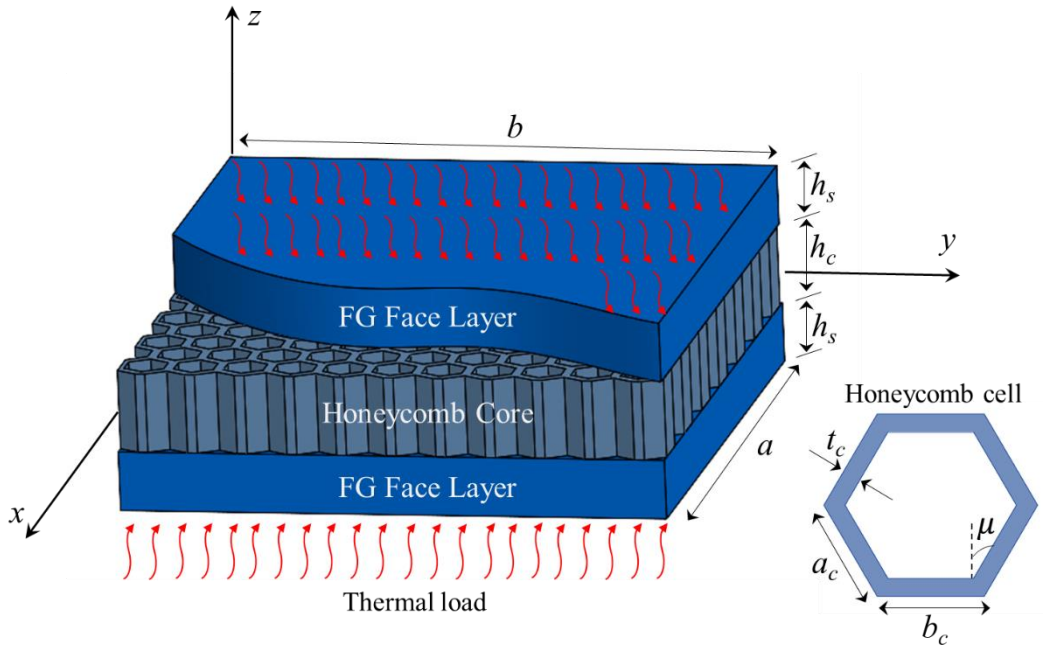

Figure 1. A honeycomb core sandwich plate composed of FG face layers.

2.2. Honeycomb cell configuration

The four factors determining the features of every honeycomb unit are length of the inclined cell rib a_c, angle of inclination μ, rib thickness t_c, and length of the horizontal cell rib b_c. SUS304 is preferred for the honeycomb plate due to its mechanical and thermal characteristics. Gibson's approach can be used to calculate the hexagonal honeycomb plate's equivalent material characteristics with the formulation that follows [28,29]:

$$E_{11}^{C} = \frac{E_{SUS304}\xi^3 \cos\mu}{(\psi + \sin\mu)\sin^2\mu}[1 - \xi^2 \cot^2\mu] \quad (1)$$

$$E_{22}^{C} = \frac{E_{SUS304}\xi^3(\psi + \sin\mu)}{cos^3\,\mu}[1 - \xi^2(\psi\, sec^2\,\mu + tan^2\,\mu)] \quad (2)$$

$$E_{33}^{C} = \frac{E_{SUS304}\xi(2 + \psi)}{2(\psi + \sin\mu)\cos\mu} \quad (3)$$

$$G_{12}^{C} = \frac{E_{SUS304}\xi^3(\Omega + \sin\mu)}{\psi^2(1 + 2\psi)\cos\mu} \quad (4)$$

$$G_{13}^{C} = \frac{G_{SUS304}\xi\cos\mu}{\psi + \sin\mu} \quad (5)$$

$$G_{23}^{C} = \frac{G_{SUS304}\xi}{2\cos\mu}\left[\frac{\psi + \sin\mu}{(1 + 2\psi)\cos\mu} + \frac{\psi + 2sin^2\,\mu}{2(\psi + \sin\mu)}\right] \quad (6)$$

$$\rho^{C} = \frac{\rho_{SUS304}\xi(\psi + 2)}{2\cos\mu\,(\psi + \sin\mu)} \quad (7)$$

in which $\xi = t_c/a_c$ and $\psi = b_c/a_c$. Based on the geometric variables, the corresponding coefficients for Poisson's ratio v^C, thermal expansion α^C, and thermal conductivity κ^C can be obtained in the manner shown below:

$$v_{12}^{C} = \frac{cos^2\,\mu}{(\psi + \sin\mu)\sin\mu}[1 - \xi^2\, csc^2\,\mu] \quad (8)$$

$$v_{21}^{C} = \frac{(\psi + \sin\mu)\sin\mu}{cos^2\,\mu}[1 - \xi^2(1 + \psi)\, sec^2\,\mu] \quad (9)$$

$$\alpha^{C} = \frac{\alpha_{SUS304}\xi(\psi + 2)}{2\cos\mu\,(\psi + \sin\mu)} \quad (10)$$

$$\kappa^{C} = \frac{\kappa_{SUS304}\xi(\psi + 2)}{2\cos\mu\,(\psi + \sin\mu)} \quad (11)$$

2.3. FG face layers

The core layer made of honeycomb cells is sandwiched between two FG composite plate layers. The top surface of the FGM layers is considered to be ZrO_2 and the bottom surface is considered to be SUS304. The mechanical and thermal variables of the surface layers vary uniformly throughout the z axis according to the power law distribution. The effective mechanical and thermal properties of the FGM face plates can be calculated as [30]:

$$E_{ef} = E_{ZrO_2} + \left(E_{SUS304} - E_{ZrO_2}\right)V^i \quad (i = tl, bl) \tag{12}$$

$$v_{ef} = v_{ZrO_2} + \left(v_{SUS304} - v_{ZrO_2}\right)V^i \quad (i = tl, bl) \tag{13}$$

$$\rho_{ef} = \rho_{ZrO_2} + \left(\rho_{SUS304} - \rho_{ZrO_2}\right)V^i \quad (i = tl, bl) \tag{14}$$

$$\alpha_{ef} = \alpha_{ZrO_2} + \left(\alpha_{SUS304} - \alpha_{ZrO_2}\right)V^i \quad (i = tl, bl) \tag{15}$$

$$\kappa_{ef} = \kappa_{ZrO_2} + \left(\kappa_{SUS304} - \kappa_{ZrO_2}\right)V^i \quad (i = tl, bl) \tag{16}$$

where the subscripts $SUS304$ and ZrO_2 refer to the material properties of the metal and ceramic matrix respectively, while the superscripts bl and tl represent the lower and upper FG layers. Furthermore, the ρ_{ef}, v_{ef}, α_{ef}, κ_{ef}, and E_{ef} indicate the effective properties of surface layers. The following approach can be employed to determine the volume ratio, denoted as V^i, utilizing the power-law distribution [31,32]:

$$\begin{aligned} V^{bl} &= \left(\frac{1}{2} - \frac{2z + h_c + h_s}{2h_s}\right)^n \quad h_1 \le z \le h_2 \\ V^{tl} &= \left(\frac{1}{2} + \frac{2z - h_c - h_s}{2h_s}\right)^n \quad h_3 \le z \le h_4 \end{aligned} \tag{17}$$

in which $h_1 = -h_c/2 - h_s$, $h_2 = -h_c/2$, $h_3 = h_c/2$ and $h_4 = h_c/2 + h_s$. The variable z represents the location toward the neutral axis, whereas the variable n symbolizes the power-law parameter (for $n = 0$, $v_{ef} = v_{SUS304}$ and for $n = \infty$, $v_{ef} = v_{ZrO_2}$).

The FG sandwich composite plate's physical properties change as a function of temperature. A nonlinear temperature equation can be utilized to describe the thermal and mechanical properties in the following way [33–35]:

$$P = P_0(P_{-1}T^{-1} + 1 + P_1T + P_2T^2 + P_3T^3) \tag{18}$$

where $T = T_0 + \Delta T$ and $T_0 = 300$ K. P_0, P_{-1}, P_1, P_2, and P_3 refer to the temperature-dependent material constants. The temperature is regarded as exhibiting a nonlinear change. Under certain temperature constraints, Eq. (18) can be computed to find the top and bottom layer temperatures (T_t and T_b) of the plate [36].

$$-\frac{d}{dz}\left[\kappa(z,T)\frac{dT}{dz}\right] = 0, \qquad T\left(\frac{h_c}{2} + h_s\right) = T_t, \quad T\left(-\frac{h_c}{2} - h_s\right) = T_b \tag{19}$$

where κ denotes the thermal conductivity coefficient. In addition, h_c and h_s define the core and FG layer thicknesses, respectively.

The equation that follows can be used to calculate the temperature of any place along the thickness direction [37]:

$$T(z) = T_b + \frac{(T_t - T_b)\int_{-\frac{h}{2}}^{z}\frac{1}{\kappa(z,T)}d(z)}{\int_{-\frac{h}{2}}^{\frac{h}{2}}\frac{1}{\kappa(z,T)}d(z)} \tag{20}$$

3. Results and Discussion

In this section, the variation of thermomechanical material properties (effective modulus of elasticity, Poisson's ratio, thermal expansion coefficient, and thermal conductivity coefficient) of sandwich FG honeycomb core plate are investigated under temperature loading. The simulations are based on the following nanostructure fundamental variables: $a = b = 400$ nm, $h = a/10$, $h_c = 0.6h$ and $h_s = 0.2h$. The temperature dependent mechanical and thermal properties of ZrO_2 and SUS304 ceramic-metal matrix are listed in Table 1.

Table 1. Mechanical and thermal constants of SUS304 and ZrO_2 [33], [35].

Material	Properties	P_{-1}	P_0	P_1	P_2	P_3
SUS304	E (Pa)	0	$201.04\,x10^9$	$3.079\text{x}10^{-4}$	$-6.534\text{x}10^{-7}$	0
	υ	0	0.3262	$-2.002\text{x}10^{-4}$	$3.97\text{x}10^{-7}$	0
	α ($1K^{-1}$)	0	$12.33\text{x}10^{-6}$	$8.086\text{x}10^{-4}$	0	0
	κ (W/mK)	0	15.397	$-1.264\text{x}10^{-3}$	$2.09\text{x}10^{-6}$	$-7.223\text{x}10^{-10}$
	ρ (kg/m^3)	0	8166	0	0	0
ZrO_2	E (Pa)	0	$244.27\text{x}10^9$	$-1.371\text{x}10^{-3}$	$1.214\text{x}10^{-6}$	$-3.681\text{x}10^{-10}$
	υ	0	0.2882	$1.133\text{x}10^{-4}$	0	0
	α ($1K^{-1}$)	0	$12.766\text{x}10^{-6}$	$-1.491\text{x}10^{-3}$	$1.006\text{x}10^{-5}$	$-6.778\text{x}10^{-11}$
	κ (W/mK)	0	1.70	$1.276\text{x}10^{-4}$	$6.648\text{x}10^{-8}$	0
	ρ (kg/m^3)	0	2370	0	0	0

3.1. Verification of the solution strategy

In order to prove the validity of the solution method presented in the study, a comparison is made with the existing work in the literature. The comparison study includes a comparison of the mechanical and thermal properties of a sandwich plate containing magneto-electro-elastic surface layers reported by Koç et al [38]. In the study, the core layer consists of Si_3N_4/SUS304 ceramic-metal matrix, while the surface layers consist of 50% $BaTiO_3$ and 50% $CoFe_2O_4$. The plate dimensions and material properties are based on the reference study. The effective modulus of elasticity (E) and effective thermal conductivity coefficient (κ) are compared for two different temperature rise values and four different power law parameters. As shown in Table 2, the results of the reference study and the present study are very close.

Table 2. Comparison of the effective material properties (E and κ).

		E (Pa)		κ (W/mK)	
ΔT	n	Ref. [38]	Present	Ref. [38]	Present
400	0	$2.97\text{x}10^{11}$	$2.92\text{x}10^{11}$	$0.89\text{x}10^{-5}$	$0.93\text{x}10^{-5}$
	0.5	$2.68\text{x}10^{11}$	$2.61\text{x}10^{11}$	$1.11\text{x}10^{-5}$	$1.17\text{x}10^{-5}$
	1	$2.52\text{x}10^{11}$	$2.44\text{x}10^{11}$	$1.23\text{x}10^{-5}$	$1.29\text{x}10^{-5}$
	5	$2.23\text{x}10^{11}$	$2.16\text{x}10^{11}$	$1.45\text{x}10^{-5}$	$1.53\text{x}10^{-5}$
600	0	$2.88\text{x}10^{11}$	$2.83\text{x}10^{11}$	$1.09\text{x}10^{-5}$	$1.18\text{x}10^{-5}$
	0.5	$2.58\text{x}10^{11}$	$2.52\text{x}10^{11}$	$1.34\text{x}10^{-5}$	$1.42\text{x}10^{-5}$
	1	$2.42\text{x}10^{11}$	$2.33\text{x}10^{11}$	$1.46\text{x}10^{-5}$	$1.61\text{x}10^{-5}$
	5	$2.14\text{x}10^{11}$	$2.04\text{x}10^{11}$	$1.71\text{x}10^{-5}$	$1.88\text{x}10^{-5}$

3.2. Effective thermomechanical material properties of the honeycomb sandwich structure

In this subsection, variation of thermomechanical material properties (E, υ, α and κ) of sandwich FG honeycomb core plate with respect to temperature rise (ΔT), power law distribution (n) and honeycomb geometrical parameters (ψ, ξ and μ) are investigated in the range of 0-1000 K. Analytical examinations are performed for four distinct power law constants (n=0, 1, 2, and 10). While FG surface layers exhibit completely SUS304 properties at n=0, the plate properties approach ZrO_2 with increasing

n. The analyses are carried out by considering the thickness-to-length of the inclined cell rib ratio $\xi = 0.025, 0.1\ 0.2$ and 0.3, length of the horizontal cell rib-to-length of the inclined cell rib ratio $\psi = 0.5, 1, 2$ and 4 and inclination angle $\mu = 30^o, 45^o$ and 60^o.

Figure 2 presents the variation of the equivalent effective elastic modulus of the sandwich plate with respect to ΔT, n, ψ, ξ and μ. As shown in Figure 2a, E decreases nonlinearly with increasing ΔT. In addition, the equivalent modulus of elasticity of the sandwich plate decreases significantly with increasing n. This decrease is due to the difference in E value of ZrO_2 and SUS304. When Table 1 is examined, it is seen that the P_0 value of ZrO_2 is higher than SUS304. Accordingly, the initial values of the $n = 10$ curve should be higher than the $n = 0$ curve. However, since the young modulus of ZrO_2 decreases much faster than SUS304 at low temperatures, the $n = 10$ curve is positioned lower than the $n = 0$ curve. As shown in Figure 2b, Figure 2c and Figure 2d, the modulus of elasticity of the sandwich plate decreases with increasing ψ and μ, while it increases with increasing ξ. From the evaluation of the figures, it is concluded that the n parameter affects the equivalent effective E value of the plate the most and the ψ parameter the least.

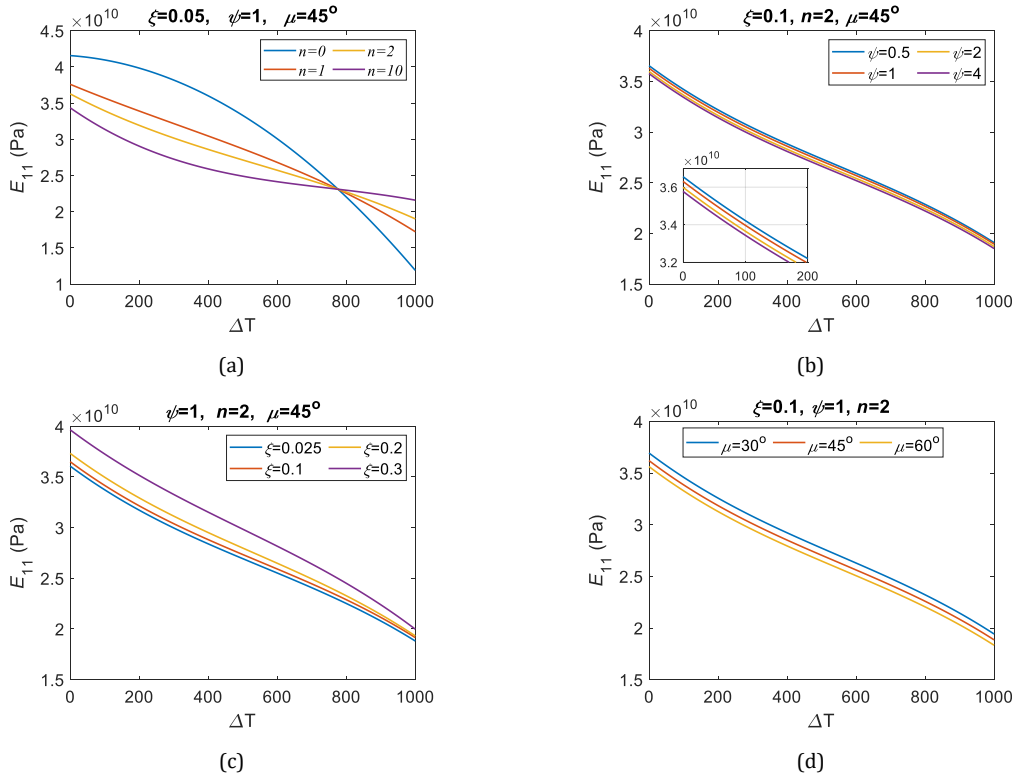

Figure 2. Variation of the effective modulus of elasticity E_{11} with respect to ΔT, n, ψ, ξ and μ parameters.

The variation of the equivalent effective Poisson's ratio v_{12} of the sandwich plate with respect to parameters ΔT, n, ψ, ξ and μ is depicted in Figure 3. As shown in Figure 3a, v_{12} increases nonlinearly with increasing ΔT, while it decreases with increasing n. The reason for the rise in v_{12} is the softening behavior of the plate with increasing ΔT, while the reason for the decrease is that the ZrO_2 composition in the plate becomes more dominant with increasing n. As shown in Figure 3b, Figure 3c and Figure 3d, increasing ψ, ξ and μ have a decreasing effect on the effective v_{12} value. From the detailed examination of the figures, it is determined that the parameters n and ΔT affect the effective Poisson's ratio less than the geometrical parameters ψ, ξ and μ. It is also shown that ψ and μ are the dominant parameters in determining the effective v_{12}. For example, considering the curves $\psi = 0.5$ and $\psi = 4$, it is seen that there is an increase of about 159.88% at $\Delta T = 1000$ K.

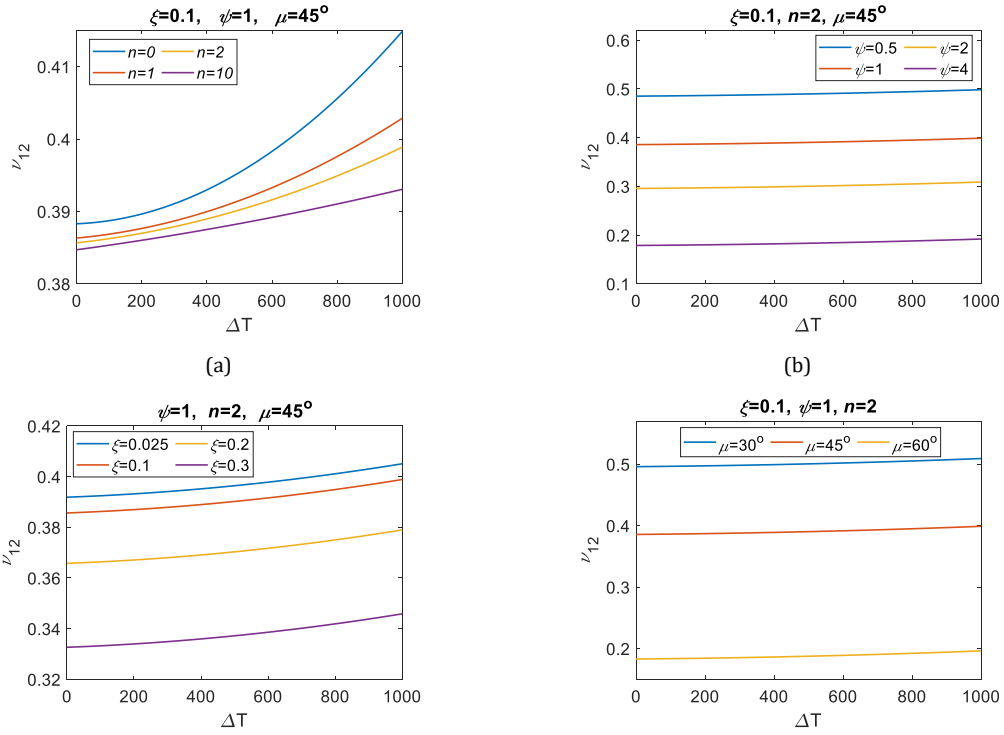

Figure 3. Variation of the effective Poisson's ratio v_{12} depending on the ΔT, n, ψ, ξ and μ parameters.

Figure 4 graphically illustrates the variations of the coefficient of effective thermal expansion α of the sandwich plate with respect to parameters ΔT, n, ψ, ξ and μ. As depicted in Figure 4a, increasing ΔT and n have an increasing effect on the effective α coefficient of the sandwich plate. The reason for this increase is attributed to the softening tendency of the plate with rising ΔT and the increase in the ZrO_2 ratio in the surface layers with increasing n. As given in Table 1, although the thermal expansion coefficients of SUS304 and ZrO_2 at low temperatures are close to each other, there is a significant difference between the $n = 0$ and $n = 10$ curves in Figure 4a. The reason for this difference is attributed to the superior thermal expansion properties of ZrO_2 at high temperatures and the rapid increase in α. Furthermore, as depicted in Figure 4b, Figure 4c and Figure 4d, increasing ξ and μ have an increasing effect on α coefficient, whereas increasing ψ has a decreasing effect. It can be concluded from Figure 4 that the honeycomb geometrical parameters affect the α values less than ΔT and n and that ΔT has the highest effect on the change in the thermal expansion coefficient and ψ has the least.

The variation of the equivalent effective thermal conductivity coefficient of the sandwich plate with respect to parameters ΔT, n, ψ, ξ and μ is evaluated in Figure 5. As indicated in Figure 5a, κ increases with rising ΔT while κ decreases with increasing n. When $n = 0$ and $n = 10$ curves are examined, it is seen that κ decreases from 4.416 1/K to 2.088 1/K at ΔT =500 K. That is, a decrease of 111.494%. The reason for these decreases is the superior thermal conductivity of SUS304 compared to ZrO_2 and the fact that ZrO_2 is not affected much by the temperature rise. Furthermore, as shown in Figures 5b, 5c and 5d, ξ and μ show a similar trend, leading to an increase in κ, while increasing ψ has the inverse effect, leading to a decrease in κ.

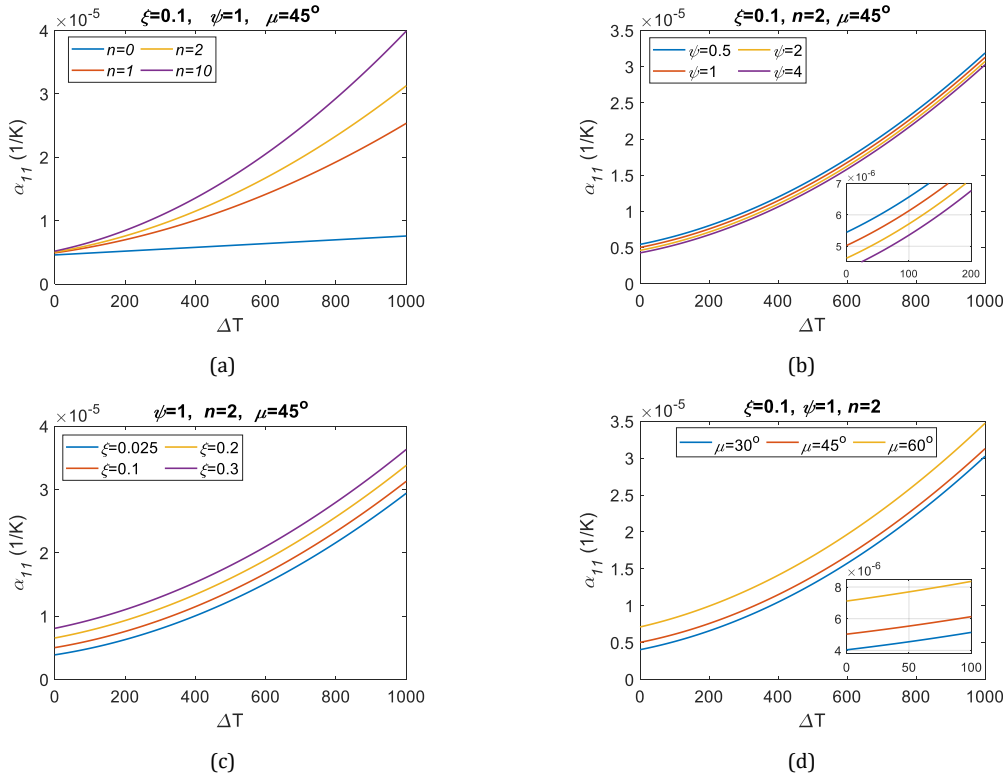

Figure 4. Variation of the effective coefficient of thermal expansion α_{11} with respect to ΔT, n, ψ, ξ and μ parameters.

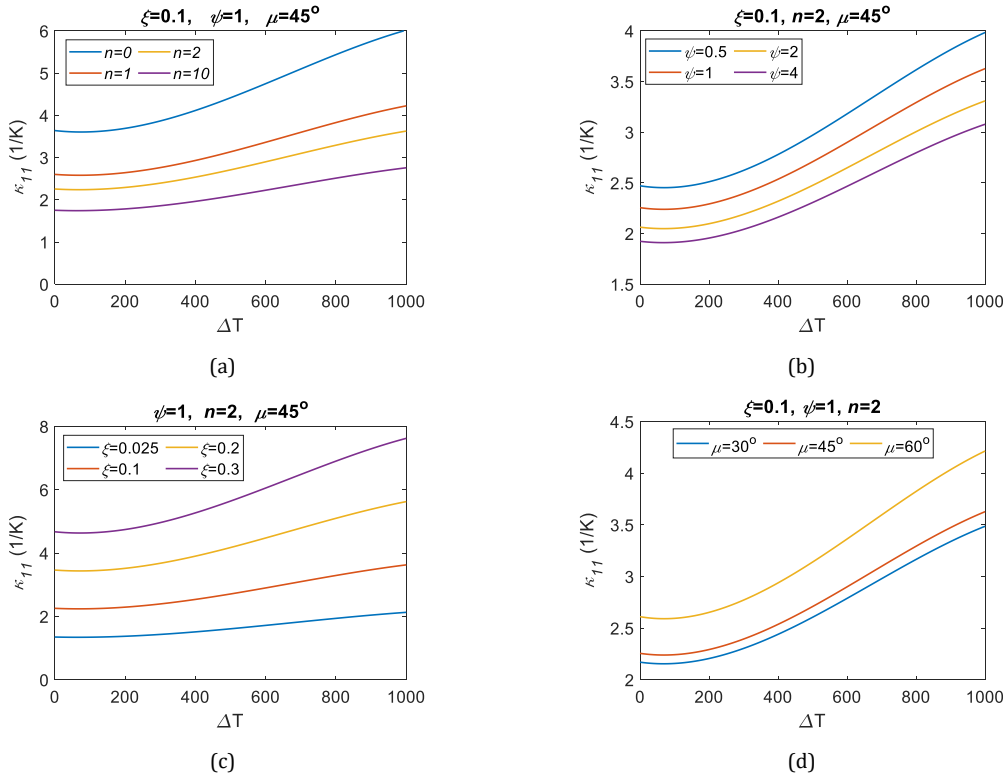

Figure 5. Variation of the effective coefficient of thermal conductivity κ_{11} depending on the ΔT, n, ψ, ξ and μ parameters.

4. Conclusions

In this paper, the variation of thermomechanical characteristics of sandwich structure with honeycomb plate and ceramic-metal matrix FGM surface layers are investigated with respect to variables such as

temperature rise, power law index and geometrical parameters of honeycomb cells. To determine the effective equivalent material characteristics of the sandwich plate, power law equations are employed for FG surface layers, while Gibson equations based on the geometric dimensions of hexagonal cells are employed for the honeycomb core. According to the parametric analyses, some important outcomes are obtained. When the effect of ΔT, n, ψ, ξ and μ parameters on the effective E value of the sandwich plate is examined, it is determined that E decreases with increasing ΔT, n and ψ, whereas it increases with increasing ξ. Furthermore, it has been found that the parameter providing the greatest influence on the modulus of elasticity of the sandwich plate is the ΔT, whereas the parameter with the least impact is ψ. From the effective Poisson's ratio plots, it is seen that the Poisson's ratio decreases with increasing n, ψ, ξ and μ parameters but decreases with increasing ΔT. In addition, when the percentage increases and decreases of the Poisson's ratio of the sandwich structure are examined, it is determined that honeycomb cell parameters are more dominant than the other parameters. Parameters ΔT, n, ξ and μ increase the coefficient of thermal expansion of the sandwich plate with a similar trend, while increasing ψ decreases α. Moreover, the most effective parameter in the variation of the α parameter of the sandwich plate is ΔT while the least effective parameter is ψ. From the examination of the thermal conductivity curves, it is inferred that the κ coefficient decreases with increasing n and ψ parameters and increases with increasing ξ and μ values. The thermomechanical characteristics of sandwich plates including a honeycomb core can be improved via selection of materials and structural design, enabling efficient thermal and mechanical management in high-temperature, noise, and corrosion environments. The results are expected to contribute to the gap in the literature on the current research topic.

Conflict of Interest Statement

The authors declare that there is no conflict of interest

References

[1] L. Ai and X. Gao, "Metamaterials with negative Poisson's ratio and non-positive thermal expansion," *Composite Structures*, vol. 162, pp. 70–84, 2017. doi:10.1016/j.compstruct.2016.11.056

[2] W. Zhang, S. Zhao, F. Scarpa, J. Wang, and R. Sun, "In-plane mechanical behavior of novel auxetic hybrid metamaterials," *Thin-Walled Structures*, vol. 159, pp. 107191, 2021. doi:10.1016/j.tws.2020.107191

[3] K. G. Aktaş, "Three-dimensional thermomechanical wave propagation analysis of sandwich nanoplate with graphene-reinforced foam core and magneto-electro-elastic face layers using nonlocal strain gradient elasticity theory," *Acta Mechanica*, vol. 235, no. 9, pp. 5587–5619, 2024. doi:10.1007/s00707-024-04001-1

[4] W. Zhang, Z. Li, J. Wang, F. Scarpa, and X. Wang, "Mechanics of novel asymmetrical re-entrant metamaterials and metastructures," *Composite Structures*, vol. 291, pp. 115604, 2022. doi:10.1016/j.compstruct.2022.115604

[5] Y. Chen, Z. Jia, and L. Wang, "Hierarchical honeycomb lattice metamaterials with improved thermal resistance and mechanical properties," *Composite Structures*, vol. 152, pp. 395–402, 2016. doi:10.1016/j.compstruct.2016.05.048

[6] K. Billon *et al.*, "Mechanics and band gaps in hierarchical auxetic rectangular perforated composite metamaterials," *Composite Structures*, vol. 160, pp. 1042–1050, 2017. doi:10.1016/j.compstruct.2016.10.121

[7] M. Eroğlu, İ. Esen, and M. A. Koç, "Managing the surface piezoelectricity effect of the smart ZnO sandwich nanoplates using metal foam core layer and GPRL reinforced rim layers," *Microsystem Technologies*, 2024. doi:10.1007/s00542-024-05772-2

[8] M. Eroğlu, İ. Esen, and M. A. Koç, "Effect of the magnetic field on the thermomechanical flexural wave propagation of embedded sandwich nanobeams," *Mechanics Based Design of Structures and Machines*, vol. 52, no. 10, pp. 7795–7827, Oct. 2024. doi:10.1080/15397734.2024.2308659

[9] A. H. Abdulaziz, M. Hedaya, A. Elsabbagh, K. M. Holford, and J. McCrory, "Acoustic emission wave propagation in honeycomb sandwich panel structures," *Composite Structures*, vol. 277, pp. 114580, 2021. doi:10.1016/j.compstruct.2021.114580

[10] E. Zurnacı and H. K. Özdemir, "Investigation of the compressive strength, energy absorption properties and deformation modes of the reinforced core cell produced by the FDM method," *Gazi Journal of Engineering Sciences*, vol. 9, no. 1, pp. 1–11, 2023. doi:10.30855/gmbd.0705047

[11] Y. Tao, M. Chen, H. Chen, Y. Pei, and D. Fang, "Strain rate effect on the out-of-plane dynamic compressive behavior of metallic honeycombs: Experiment and theory," *Composite Structures*, vol. 132, pp. 644–651, 2015. doi:10.1016/j.compstruct.2015.06.015

[12] J. Zhang, Z. Yan, and L. Xia, "Vibration and flutter of a honeycomb sandwich plate with zero Poisson's ratio," *Mathematics*, vol. 19, no. 9, pp. 2528, 2021. doi:10.3390/math9192528

[13] M. F. Sarıbaş and S. Karadeniz, "Bir uçak kanadının hücum kenarına kuş çarpmasının düzgün parçacık hidrodinamiği yöntemiyle sayısal incelenmesi," *Gazi Journal of Engineering Sciences*, vol. 8, no. 3, pp. 547–566, 2021. doi:10.30855/gmbd.0705042

[14] H. L. Tan, Z. C. He, K. X. Li, E. Li, A. G. Cheng, and B. Xu, "In-plane crashworthiness of re-entrant hierarchical honeycombs with negative Poisson's ratio," *Composite Structures*, vol. 229, p. 111415, 2019. doi:10.1016/j.compstruct.2019.111415

[15] N. V Nguyen, H. Nguyen-Xuan, T. N. Nguyen, J. Kang, and J. H. Lee, "A comprehensive analysis of auxetic honeycomb sandwich plates with graphene nanoplatelets reinforcement," *Composite Structures*, vol. 259, pp. 113213, 2021. doi:10.1016/j.compstruct.2020.113213

[16] O. A. Ganilova, M. P. Cartmell, and A. Kiley, "Experimental Investigation of the thermoelastic performance of an aerospace aluminium honeycomb composite panel," *Composite Structures*, vol. 257, pp. 113159, 2021. doi:10.1016/j.compstruct.2020.113159

[17] Y. Zhou, A. Liu, Y. Xu, Y. Guo, X. Yi, and Y. Jia, "Frequency-dependent orthotropic damping properties of nomex honeycomb composites," *Thin-Walled Structures*, vol. 160, pp. 107372, 2021. doi:10.1016/j.tws.2020.107372

[18] H. Liu, E. T. Zhang, and B. F. Ng, "In-plane dynamic crushing of a novel honeycomb with functionally graded fractal self-similarity," *Composite Structures*, vol. 270, pp. 114106, 2021. doi:10.1016/j.compstruct.2021.114106

[19] A. F. Ozalp and I. Esen, "Thermal buckling response of foam core smart sandwich nanoplates with electro-elastic and magneto-strictive layers," *Acta Mechanica*, 2024. doi:10.1007/s00707-024-04155-y

[20] R. Özmen and I. Esen, "Thermomechanical flexural wave propagation responses of FG porous nanoplates in thermal and magnetic fields," *Acta Mechanica*, vol. 234, no. 11, pp. 5621–5645, 2023. doi:10.1007/s00707-023-03679-z

[21] R. Özmen, R. Kılıç, and I. Esen, "Thermomechanical vibration and buckling response of nonlocal strain gradient porous FG nanobeams subjected to magnetic and thermal fields," *Mechanics of Advanced Materials and Structures*, vol. 31, no. 4, pp. 834–853, 2024. doi:10.1080/15376494.2022.2124000

[22] P. Chen, S. Chen, and Z. Peng, "Thermo-contact mechanics of a rigid cylindrical punch sliding on a finite graded layer," *Acta Mechanica*, vol. 223, no. 12, pp. 2647–2665, 2012. doi:10.1007/s00707-012-0732-y

[23] Y. Z. Wang, D. Liu, Q. Wang, and J. Zhou, "Asymptotic analysis of thermoelastic response in functionally graded plate subjected to a transient thermal shock," *Composite Structures*, vol. 139, pp. 233–242, 2016. doi:10.1016/j.compstruct.2015.12.014

[24] W. Zhou, R. Zhang, S. Ai, R. He, Y. Pei, and D. Fang, "Load distribution in threads of porous metal–ceramic functionally graded composite joints subjected to thermomechanical loading," *Composite Structures*, vol. 134, pp. 680–688, 2015. doi:10.1016/j.compstruct.2015.08.113

[25] N. D. Duc *et al.*, "Mechanical and thermal stability of eccentrically stiffened functionally graded conical shell panels resting on elastic foundations and in thermal environment," *Composite Structures*, vol. 132, pp. 597–609, 2015. doi:10.1016/j.compstruct.2015.05.072

[26] Y. L. Chung, "Thermoelastic closed-form solutions of FGM plates subjected to temperature change in longitudinal and thickness directions," *Meccanica*, vol. 57, pp. 355–369, 2022. doi:10.1007/s11012-021-01431-2

[27] A. Hajlaoui, A. Jarraya, K. El Bikri, and F. Dammak, "Buckling analysis of functionally graded materials structures with enhanced solid-shell elements and transverse shear correction," *Composite Structures*, vol. 132, pp. 87–97, 2015. doi:10.1016/j.compstruct.2015.04.059

[28] L. J. Gibson and M. F. Ashby, Cellular Solids: *Structure and Properties*, 2nd ed. in Cambridge solid state science series. Cambridge University Press, 1997.

[29] M. Sobhy and F. H. H. Al Mukahal, "Wave dispersion analysis of functionally graded GPLs-reinforced sandwich piezoelectromagnetic plates with a honeycomb core," *Mathematics*, vol. 10, no. 17, 2022. doi:10.3390/math10173207

[30] Y. Amini, H. Emdad, and M. Farid, "Finite element modeling of functionally graded piezoelectric harvesters," *Composite Structures*, vol. 129, pp. 165–176, 2015. doi:10.1016/j.compstruct.2015.04.011

[31] H. T. Thai and D. H. Choi, "A simple first-order shear deformation theory for the bending and free vibration analysis of functionally graded plates," *Composite Structures*, vol. 101, pp. 332–340, 2013. doi:10.1016/j.compstruct.2013.02.019

[32] M. Nouraei, V. Zamani and Ö. Civalek, "Vibration of smart sandwich plate with an auxetic core and dual-FG nanocomposite layers integrated with piezoceramic actuators," *Composite Structures*, vol. 315, pp. 117014, 2023. doi:10.1016/j.compstruct.2023.117014

[33] Y. S. Touloukian, *Thermophysical properties of high temperature solid materials.* New York: Macmillan, 1967.
[34] Y. S. Touloukian, Thermophysical properties of high temperature solid materials: *Oxides and their solutions and mixtures.* New York: Macmillan, 1966.

[35] J. N. Reddy and C. D. Chin, "Thermomechanical analysis of functionally graded cylinders and plates," *Journal of Thermal Stresses*, vol. 21, no. 6, pp. 593–626, 1998. doi:10.1080/01495739808956165

[36] D. G. Zhang, "Thermal post-buckling and nonlinear vibration analysis of FGM beams based on physical neutral surface and high order shear deformation theory," *Meccanica*, vol. 49, no. 2, pp. 283–293, 2014. doi:10.1007/s11012-013-9793-9

[37] F. Ebrahimi and M. R. Barati, "Electromechanical buckling behavior of smart piezoelectrically actuated higher-order size-dependent graded nanoscale beams in thermal environment," *International Journal of Smart and Nano Materials*, vol. 7, no. 2, pp. 69–90, 2016. doi:10.1080/19475411.2016.1191556

[38] M. A. Koç, İ. Esen, and M. Eroğlu, "Thermomechanical vibration response of nanoplates with magneto-electro-elastic face layers and functionally graded porous core using nonlocal strain gradient elasticity," *Mechanics of Advanced Materials and Structures*, vol. 31, no. 18, pp. 4477–4509, 2023. doi:10.1080/15376494.2023.2199412